ACS APPLIED MATERIALS & INTERFACES

Research Article

www.acsami.org

Self-healing Encapsulation Strategy for Preparing Highly Stable, Functionalized Quantum-Dot Barcodes

Tao Song,[†,§,⊥] Junqing Liu,[†,⊥] Wenbin Li,[‡] Yunhong Li,[†] Qiuhua Yang,[†] Xiaoqun Gong,[†] Lixue Xuan,*[,‡] and Jin Chang*[,†]

[†]Institute of Nanobiotechnology, School of Materials Science and Engineering, Tianjin University and Tianjin Key Laboratory of Composites and Functional Materials, Tianjin, 300072, P.R. China

[‡]Cancer Hospital, Chinese Academy of Medical Sciences & Peking Union Medical College, Beijing, 100021, P.R. China

[§]National Engineering Technology Research Center For SCRF, Linyi, 276700, P.R. China

Supporting Information

ABSTRACT: Quantum dot (QD) barcodes are becoming an urgent requirement for researchers and clinicians to obtain high-density information in multiplexed suspension (bead-based) assay. However, how to improve the stability of quantum dot barcodes is a longstanding issue. Here, we present a new self-healing encapsulation strategy to generate functionalized uniform quantum dots barcodes with high physical and chemical stability. This efficient and facile strategy could make porous polymer microspheres self-heal to encapsulate QDs via the thermal motion and interaction of the molecular chains. Consequently, the new strategy solved especially the QDs leakage problem and improved the chemical stability under different pH physiological conditions as well as the longtime storage stability. In the meantime, the encoding capacity and the spatial distribution uniformity of quantum dots could be also improved. Furthermore, immunofluorescence assays for alpha fetoprotein (AFP) detections indicated that carboxyl groups on the surface of QD-encoded microspheres could facilitate efficient attachment of biomacromolecules.

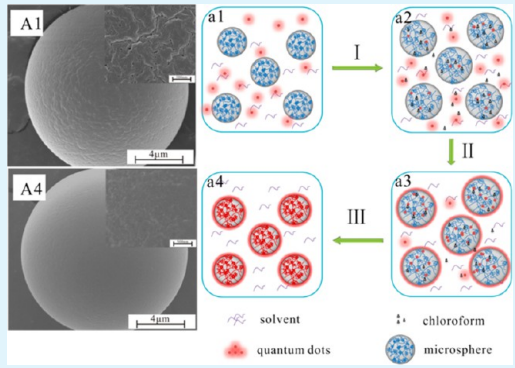

KEYWORDS: *self-healing encapsulation, high stability, quantum dot barcodes, functionalization, AFP detections*

1. INTRODUCTION

The ability to simultaneously quantify multiple molecular targets in a single sample (multiplexed analysis) is becoming an urgent requirement for researchers and clinicians to obtain high-density information with minimal assay time, sample volume, and cost.[1−3] Among the two categories of multiplexed analysis including planar arrays and suspension arrays, suspension arrays based on encoded microspheres offer various advantages. These advantages include fast solution kinetics, ease of assay modification, and higher sample throughput and superior detection sensitivity over planar arrays.[4,5]

The barcodes of microspheres applied in suspension arrays is the crucial technology of multiplexed suspension arrays. Currently, the barcode schemes can be classified as physical,[6−8] graphical,[1,9,10] electronic,[11] or spectrometric.[12−19] Among all of the barcode schemes, the fluorescent barcodes based on spectrometric technology become the popular platform technology for multiplexing due to its simple encoding process, large encoding capacity, high detection sensitivity and rapid signal acquisition. As the Luminex system demonstrated, polymer microspheres can be encoded with organic fluorescent dye to generate a library of fluorescent barcodes. However, organic dye-encoded microspheres have some limitations, such as photobleaching, the narrow excitation spectra, and broad emission spectrum. Quatum dots (QDs) have been increasing in use a natural substitutes for organic dyes to encode polymer microspheres due to their excellent and unique optical properties including high quantum yield, good photostability, broad excitation spectra, their sharp and symmetrical fluorescent peak, and the fact that differently sized QDs can be excited simultaneously by a single wavelength.[12−15] Using solution chemistry, different approaches have been used to produce QDs-encoded microspheres. Typically, the microspheres act as a carrier, and quantum dots as guests can be encapsulated into the microspheres,[12−17,20] incorporated during the microsphere synthesis,[18,21−23] or immobilized on the microspheres surface by a layer-by-layer (LBL) adsorption technique.[19,20,24] Multiple quantum dots have been embedded into a polymer microparticle in a precisely defined ratio creating a larger number of unique emission spectra.[12−17] In theory, the use of six colors and ten intensity levels can theoretically encode one million biomolecules.

Received: November 21, 2013
Accepted: February 4, 2014
Published: February 4, 2014

   dx.doi.org/10.1021/am405285u | ACS Appl. Mater. Interfaces 2014, 6, 2745−2752

Despite the fact that much progress has been made, a number of notable challenges associated with QD-encoded microspheres still exist, such as reduced reproducibility in manufacturing the individual encoded particles in large numbers and QDs leaching from encoded microspheres in medium- and chemical-induced degradation (e.g., spectral shift and intensity variation), which may lead to signal fluctuation of QD encoding. Therefore, how to fabricate uniform QD-encoded beads with high stability for accurate suspension assays becomes the focused question.[2,5,18,21,22,25−27] Here, we presented a new self-healing encapsulation strategy to incorporate QDs into high cross-linked porous polymer microspheres—utilizing microspheres to confine hydrophobic QDs via the self-healing encapsulation strategy. This efficient and facile process resulted in a uniform QD spatial distribution, larger QD loading capacity, and especially highly stable quantum-dot barcodes. We expect the self-healing encapsulation strategy will open exciting opportunities for highly stable quantum-dot barcodes to realize quantitative multiplexed analysis, and this strategy can be also adapted to other systems.

2. EXPERIMENTAL SECTION

2.1. Materials. Styrene (99%), ethyleneglycol dimethacrylate (EGDMA, 98%), poly(vinylpyrrolidone) (PVP K-40), and sodium dodecyl sulfate (SDS) were purchased from Sigma-Aldrich Corp. Benzoyl peroxide (BPO), methacrylic acid (MAA, 98%), and polyvinyl alcohol (PVA, M_w = 130 000) were obtained from Fluca. Cadmium oxide (CdO, 99.99%, powder), zinc acetate (99.9%, powder), selenium (Se, 99.9%, powder), sulfur (S, 99.9%, powder), trioctylphosphine (TOP, 90%), oleic acid (OA, 90%) and 1-octadecene (ODE, 90%) were purchased from Aldrich. FITC-labeled anti-AFP (alpha fetoprotein) was provided by Beijing Dingguo Biotechnology Co. Ltd. (China). All other chemicals were of analytical grade and obtained from local suppliers.

2.2. Equipment. The fluorescence spectra of QDs-encoded microspheres were achieved with a luminescence spectrometer (F-280, Tianjin GangDong Technology development Co., Ltd., China) and a fiber optic spectrometer (AvaSpec-2048, Avantes, Netherlands). True-color fluorescence images were obtained with an inverted Olympus microscope (IX-51), an Olympus Micro DP-72 camera, a broad-band ultraviolet (330−385 nm) light source (100-W mercury lamp) and a long-pass interference filter (DM 400, Chroma Tech, Brattleboro, VT). The confocal fluorescence cross-section images at different focalized planes from the top to the bottom of the bead were obtained with a fluorescent confocal microscope (Fluo View 1000, Olympus Inc., Japan). The morphology images of the polymer microspheres were obtained with scanning electron microscopy (SEM, XL-30, Philips Corp.).

2.3. Preparation of Monodisperse Highly Cross-Linked Porous Carboxylic Polystyrene Microspheres. Monodisperse highly cross-linked porous poly(styrene-*co*-EGDMA-*co*-MAA) microspheres were prepared by a modified two-step seeded polymerization. The seed latex particles were prepared according to our previous reports.[27] The typical seeded polymerization was shown as follows: First, the seed particles and cyclohexane were dispersed in 0.25 wt % SDS aqueous solution, stirring for 10 h at 30 °C. Second, styrene, EGDMA (100 wt %), MAA (10 wt %), toluene (100 wt %), and BPO (1 wt %) was emulsified in 0.25 wt % SDS solution by ultrasonic before added into the reactor (all of these agents were measured relative to monomer). Finally, 2.5 wt % PVA aqueous solution and copper chloride were poured into the reactor after 12 h. Then, the system temperature was raised and kept at 80 °C for 10−12 h. The final beads were obtained by repeated centrifugation and washing for several times in ethanol/water solution.

2.4. Preparation of $Cd_{1-x}Zn_xSe_{1-y}S_y$ QDs. $Cd_{1-x}Zn_xSe_{1-y}S_y$ QDs were prepared according to a previous method published by Bae et al.[28] Briefly, CdO, zinc acetate, oleic acid, and 1-octadecne were mixed, and then heated to 150 °C under Ar gas atmosphere for 20 min. The mixture was further heated to 310 °C to form a clear solution of $Cd(OA)_2$ and $Zn(OA)_2$. At this temperature, Se powder and S powder both dissolved in TOP were quickly injected into the reaction flask. After the injection, the temperature of the reaction system was set to 300 °C for 10 min and then cooled to room temperature. QDs were purified by chloroform and an excess amount of acetone.

2.5. Preparation of QD-Encoded Microspheres by the Self-healing Encapsulation Strategy. The self-encapsulation strategy was carried out in a three-neck flask equipped with condensation tube, magnetic stirrer, and argon shield. The process is briefly described as follows: (1) QDs were dispersed in chloroform (0.5−2 mL), and polymer microspheres were dispersed in hexadecane (3−5 mL). Then, the mixture was fully dispersed by ultrasound, poured into the reaction, and stirred at 50 °C for 1−2 h. (2) The temperature was slowly raised to 180 °C and kept warm until disappearance of condensing reflux; then it was cooled rapidly to room temperature. The argon protection ran through the entire process. The final microspheres were obtained by repeated centrifugation and washing several times with ethanol/cyclohexane (1:1, v/v).

2.6. QD-Encoded Microsphere-Based Sandwich Immunoassays. QD-encoded microspheres first were attached with AFP capture antibody with EDC and NHS as activators. The microspheres, EDC, and NHS were mixed in MES solution successively to activate for 20 min. The microspheres were then washed with PBS (pH 7.4). AFP capture antibody was added into the microsphere PBS solution. After incubation of 2.5 h, the beads were washed with PBS-T (0.01 M, pH 7.4, 0.05% Tween) and then resuspended in 1 wt % BSA at 4 °C overnight to reduce nonspecific interactions.[27,29] The mass ratio of microspheres/EDC/NHS/AFP capture antibody was 1/1/2/0.2. For the immunofluorescence, both the experimental group and control group were carried out in the same manner with AFP and BSA. First, 20 mL of labeled microspheres (0.01 mg μL^{-1}) and 10 μL targets (10 mg mL^{-1}) were mixed in PBS for 30 min. Then, the particles were washed with PBS before being resuspended in PBS. Second, 50 μL FITC-labeled AFP reporter bodies (0.5 mg mL^{-1}) were added into the system. After gently mixing the solution for 30 min, the final particles were purified by centrifugation and finally dissolved in PBS to be examined.

3. RESULTS AND DISCUSSION

3.1. Design and Characterization of Quantum-Dot Barcodes by the Self-healing Encapsulation Strategy. The QD-encoded polymer microspheres are fabricated by a new self-healing encapsulation strategy as shown in Figure 1. The cross-linked porous polymer microspheres are prepared with styrene as monomer, EGDMA as cross-linker, and MAA as functional monomer by seeded polymerization. First, the QDs are fully hydrophobic and homogenously mixed with chloroform to form solution. Hexadecane is chosen as the solvent because it has a high boiling point and porous polymer microspheres are insoluble in it. Upon mixing the QD solutions with 20 mg hydrophobic porous polymer microspheres in 4 mL hexadecane, the polymer microspheres are swelled in the chloroform due to the intrinsic hydrophobic nature of polymer microspheres (I stage, swelling). After that, the mixture is gradually increased to 180 °C under an inert environment. The chains of the polymer spontaneously move during the temperature increase stage. To a certain extent, the porous microspheres continue to swell. With the evaporation of chloroform, it is easier for QDs to impregnate the porous polymer microspheres by their concentration difference between the inner and outer phases of the microspheres (stage II, temperature increase). After the system is heated to 180 °C and the chloroform is removed, the thermal motion and interaction of molecular chains lead the pores to shrink, even close. After rapid cooling, the polymer microspheres are

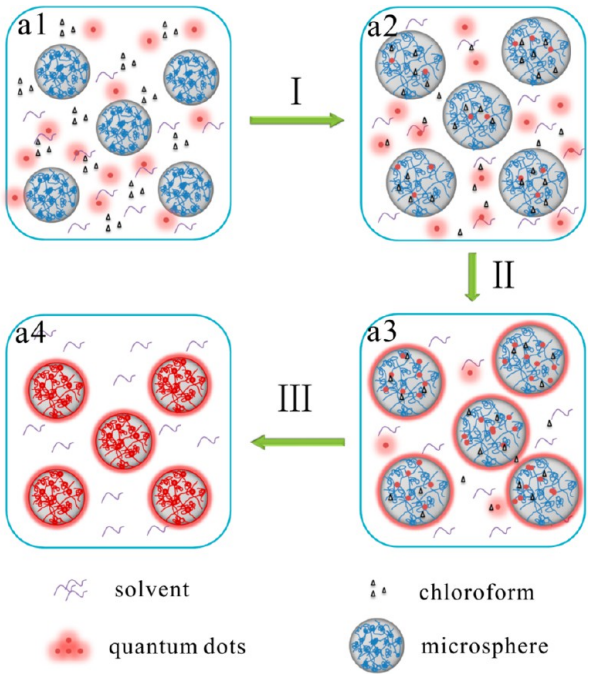

Figure 1. Schematic of the self-healing encapsulation strategy. (a1−a4) Encoding process consisting of three stages of (I) swelling, (II) temperature increase, and (III) deswelling and rapidly cooling.

deswollen and the molecular chains of the microspheres will be frozen again. (stage III, deswelling and rapidly cooling). Special internal structures of polymer microspheres simultaneously contribute to confine QDs into microspheres. Therefore, QDs can be eventually encapsulated in the polymer microspheres to avoid QD leakage from beads and reduce the effect of oxygen or solvents (such as water, PBS buffer, etc) on QDs.

The strategy that we proposed has a number of advantages over traditional solvent evaporation strategies: first, the self-healing encapsulation strategy can improve quantum dots encoding capacity. Second, new strategy has no effect on the chemical stability of QDs during the encoding process due to the organic solvent system under inert environment. Third, new strategy can improve QDs spatial distribution uniformity throughout polymer beads. Finally and most importantly, new strategies can solve the QD leakage problem from beads and improve QD-encoded beads the chemical stability due to QDs in a relatively airtight microspheres and the existence of hydrophobic interaction between QDs and polymer matrices.

We first investigated the surface properties and glass transition temperature (T_g) of the polymer microspheres to validate our the self-healing encapsulation strategy. As shown in Figure 2a1, the porous polymer microspheres are 15 μm in diameter, and their structure is obviously porous (Figure 2a1). After the self-healing encapsulation, as we expected, QD-encoded microspheres appear relatively smooth on the outer

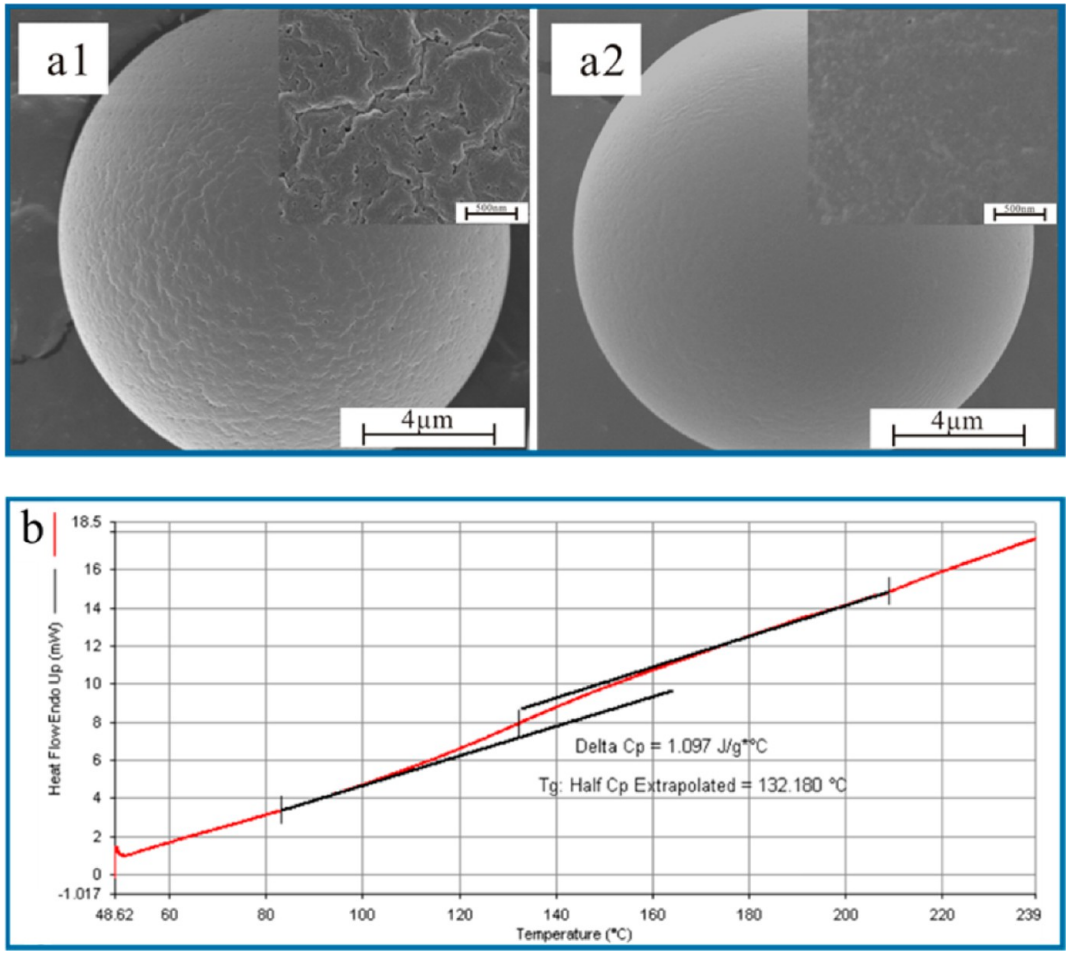

Figure 2. SEM images of the microsphere surface: original porous polymer microspheres (a1) and the QD-encoded microspheres (a2). (inset) Magnified 100 000 times. The images were taken under the same conditions. DSC curve of highly cross-linked porous polymer microspheres (b).

dx.doi.org/10.1021/am405285u | ACS Appl. Mater. Interfaces 2014, 6, 2745−2752

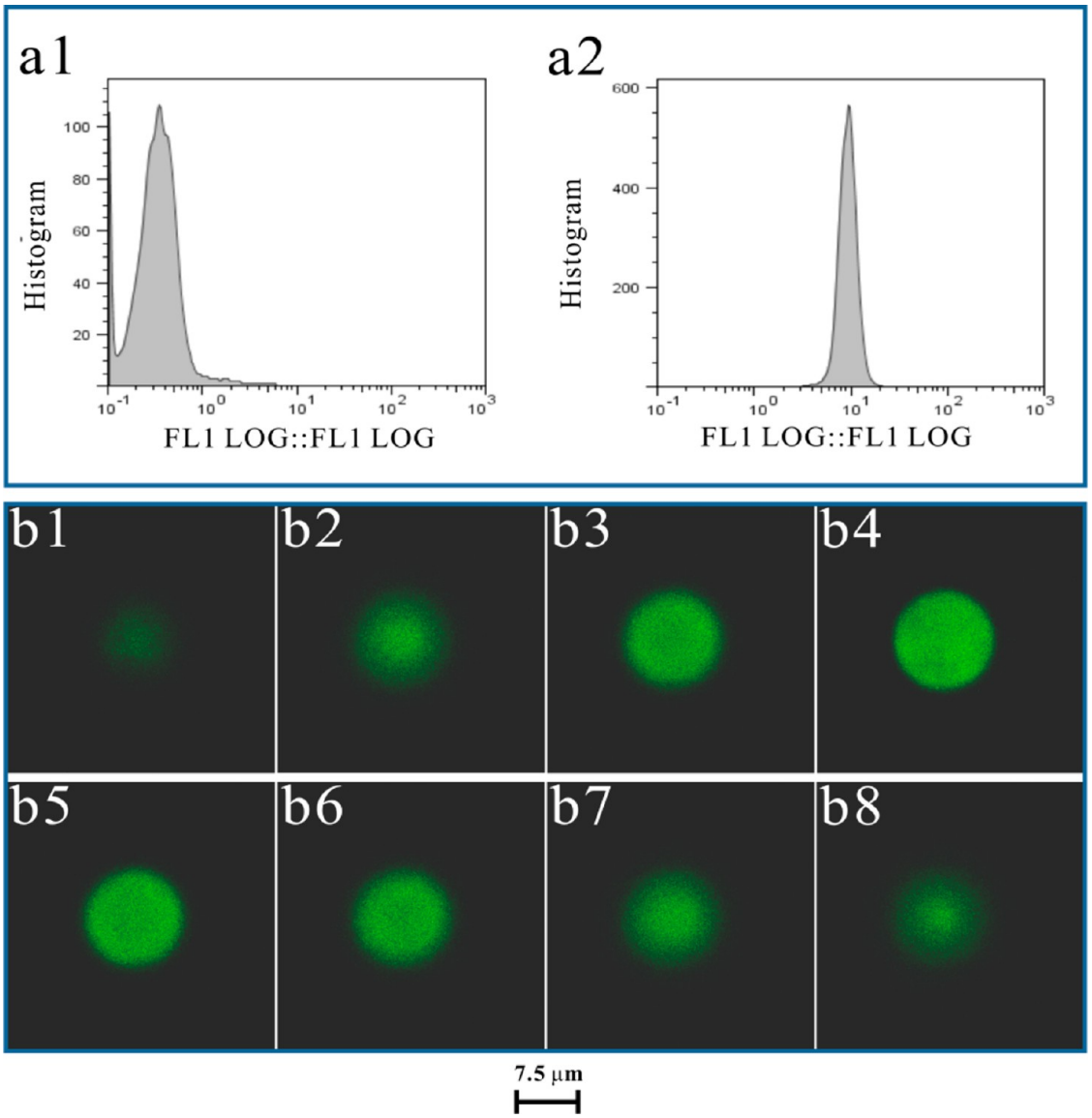

Figure 3. Fluorescence intensity comparison of the QD-encoded microspheres obtained by two methods (solvent evaporation method and the self-healing encapsulation method) in a conventional flow cytometry (a1, a2). The confocal fluorescence images of QD-encoded microspheres at different focalized planes from the top to the bottom of the bead fabricated by the self-healing encapsulation (b1−b8).

surface and no crevices or cracks are detected (Figure 2a2). In contrast, the outer porous of QD-encoded microspheres prepared via traditional solvent evaporation methods are not sealed. This is because the thermal motion and interaction of molecular chains lead to the melting procedure of polymer microspheres by raising the temperature above the T_g value, which is also confirmed by the T_g characteristic of polymer microspheres (Figure 2b).[30,31] These result indicate pores on the surface of polymer microspheres could achieve self-healing to form relatively sealed polymer shells by our new strategy.[32−34]

Quantitative flow cytometric data shown in Figure 3a1 and a2 indicate that QD barcodes fabricated by the self-healing encapsulation were more than 30 times brighter and 2.4 times more uniform in signal intensities than those made by a traditional solvent evaporation method, which have verified the first advantage mentioned above. A key factor contributing to the improved brightness is that more QDs permeated into microspheres by the swelling of porous microspheres in the high-temperature environment. Furthermore, it is evident from the confocal fluorescence images of QD-encoded microspheres at different focalized planes from the top to the bottom of the bead that the QDs have permeated into the entire microsphere and dispersed homogeneously due to the high temperature swelling of porous microspheres and concentration difference as the driving force (Figure 3b1−b8).

The self-healing encapsulation strategy for preparing quantum-dot barcodes also can accurately achieve wavelength and fluorescence intensity encoding. As shown in Figure S1, wavelength encoding with eight different emission wavelengths is remarkably distinguishable. Compared with the pure QDs, the peak profiles do not change in the staining process, but a small red shift in the photoluminescence peak position and a little change in the full width at half-maximum (fwhm) values of the emission peak are observed, which is due to the increase in the refractive index of the surrounding optical medium and the agglutination of some QDs. Figure S2 represents that the self-healing encapsulation strategy could steadily and accurately

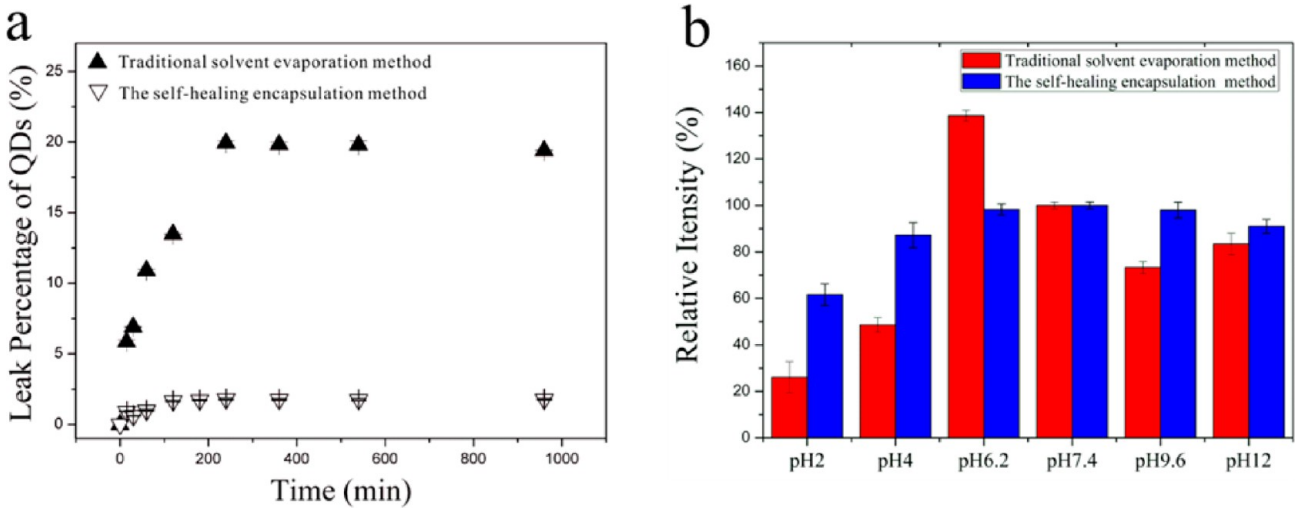

Figure 4. Contrast of organic solvent (cyclohexane) induced QDs leaching (a) and the stability in different pH aqueous solutions (b).

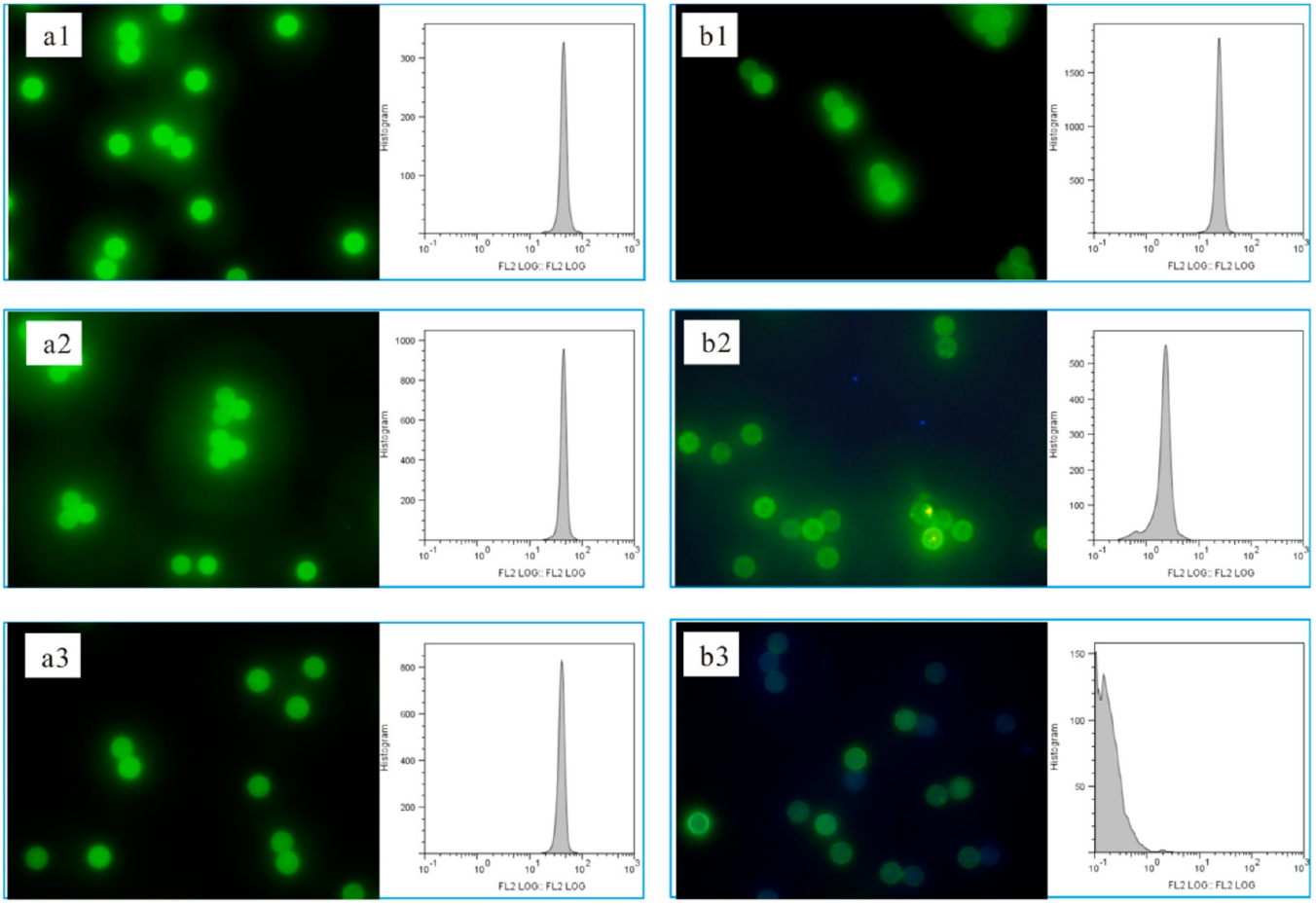

Figure 5. Temporal evolution of fluorescence images of the QD-encoded microspheres fabricated by two methods and corresponding fluorescence intensity by flow cytometry analysis. (a) Barcode by self-healing encapsulation. (b) Barcode by traditional solvent evaporation. (1) 0, (2) 3, and (3) 8 weeks.

achieve fluorescence intensity encoding, corresponding relationship curves: $y = 73.50 + 7.14x$, $R = 0.9933$.

3.2. Stability of QD-Encoded Microspheres by the Self-healing Encapsulation Strategy. Although QD-encoded microspheres have a strong fluorescent signal, a major concern in biological applications is the QD leakage from microspheres, which significantly alters the original signal of optical encoding. Here, cyclohexane which can swell the beads and also easily dissolve the QDs is used as a typical organic solvent to evaluate the leaking of encoded QDs in microspheres (Figure 4a). After the fluorescent microspheres were incubated in cyclohexane for about 12 h, quantitative spectroscopic measurements confirm that more than 20% of the embedded QDs leak out from the microspheres prepared by traditional

dx.doi.org/10.1021/am405285u | ACS Appl. Mater. Interfaces 2014, 6, 2745−2752

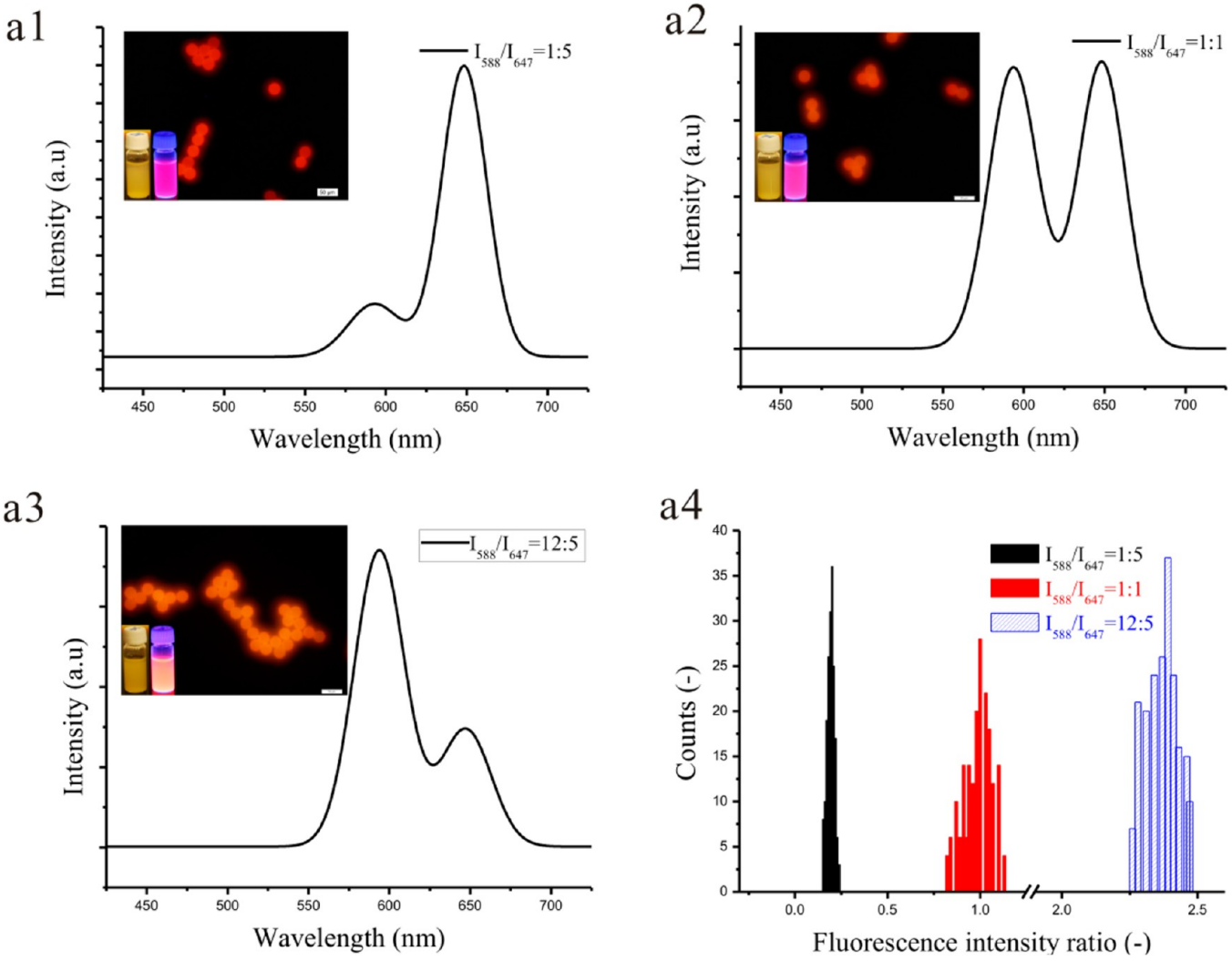

Figure 6. (a1, a2, a3) Representative single bead fluorescence spectra and the micrograph of barcodes prepared with two QDs (QD588 and QD647) by different fluorescence intensity ratio (12:5, 1:1, 1:5). The scale bar is 50 μm. (a4) Statistical distribution of three different barcodes using single bead fluorescence spectroscopy. For barcode with I_{588}/I_{647} = 12:5, the median value = 2.37, σ = 7.3%. For barcodes with I_{588}/I_{647} = 1:1 and I_{588}/I_{647} = 1:5, the median values are 0.98 and 0.19 with σ = 6.7% and 2.3%, respectively.

solvent evaporation methods, while less than 2% of QDs get out from QDs-encoded microspheres fabricated by the self-healing encapsulation. The results clearly indicate that the QD-encoded microspheres obtained by the self-healing encapsulation strategy have strong solvent resistance property and superior physical stability. Next, we also tested the chemical stability of QD-encoded microspheres under different pH physiological conditions (HCl aqueous solutions at pH 2 and 4, MES buffer at pH 6.2, PBS buffer at pH 7.4, sodium bicarbonate buffer at pH 9.6, and NaOH aqueous solutions at pH 12). The QD-encoded microspheres were challenged for 24 h, and their fluorescence intensity was measured respectively. As shown in Figure 4b, QD-encoded microspheres fabricated by the traditional solvent evaporation method are highly sensitive to the environment due to their unsealed pores. But utilizing the self-healing encapsulation, slight fluorescence fluctuation of quantum-dot barcodes is observed in aqueous solutions with pH values ranging from 2 to 12 (fluorescence at neutral pH (PBS buffer) is set to 100%). Especially in solutions of pH 5−10, the most common pH range used in bioconjugation and biomolecule detection experiments, the change of fluorescence intensity is negligible.

As a fluorescence-encoded bead-based assay product, the longtime storage of quantum-dot barcodes must be also addressed. The longtime stability of the QD-encoded microspheres in PBS (pH 7.4) was investigated by taking luminescent photographs and measuring fluorescence intensity on a flow cytometer at periodical intervals, as shown in Figure 5. It is found that there is no QD leakage from the fluorescent microspheres prepared by our approach and apparent decrease of fluorescence intensity after storage time for 8 weeks (Figure 5a1−a3). But in the case of microspheres obtained via the traditional solvent evaporation method, there appear some relatively brighter spots on the surface of microspheres over three weeks, indicating the QDs slowly leak to the outer surface from the inner pores of microspheres and agglomerate. Eight weeks later, just a few microspheres with slight fluorescence exist and the fluorescence of most microspheres disappear (Figure 5b1−b3). This illustrates that QDs diffuse out from porous microspheres and the effect of oxygen or solvents on QDs in microspheres results in a loss of barcode fluorescence intensity. Similarly, flow cytometry data indicate the same results that the microspheres prepared by our approach keep their high fluorescence intensity and display narrower

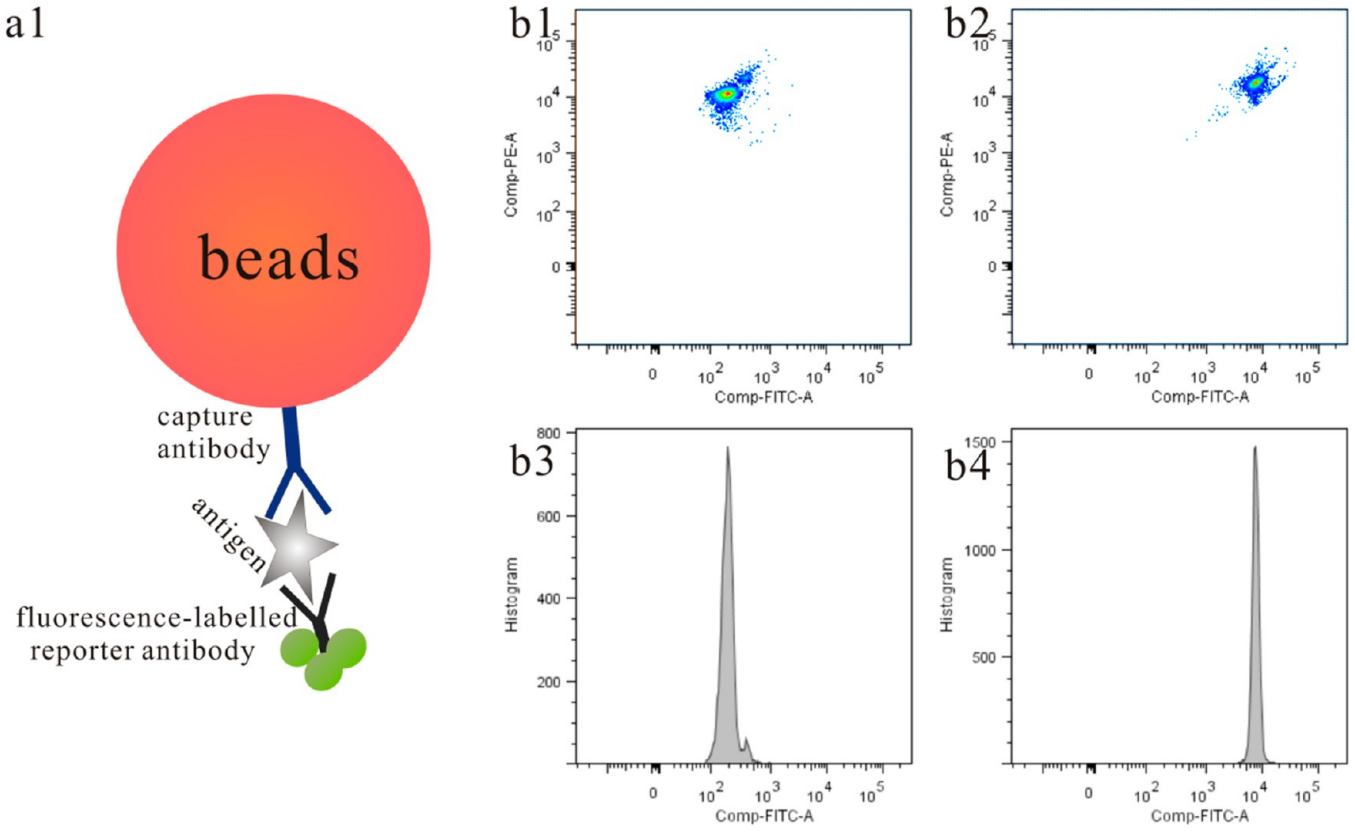

Figure 7. Principle of the immunoreactions (a1) and flow cytometry analysis of QD-encoded bead-based immunoassays (b1−b4) for AFP detection. (b1 and b3) Signal of the BSA control group. (b2 and b4) Corresponding signal of AFP group. Flow cytometric analysis was performed on a flow cytometer (Coulter, Epics XL) with a 488 nm excitation laser. Here the emission wavelength of QD-encoded microspheres is 591 nm which can be measured on the FL3 channel (PE channel) for decoding of encoded beads, and the fluorescent intensities of all samples on FL3 channel are constant. The FITC fluorescence signal was measured on the FL1 channel for the decoding of FITC-labeled AFP reporter antibody.

fluorescence distribution; however, the microspheres with unsealed pores distinctly decrease in fluorescence intensity over longtime storage in PBS medium.

On the basis of the advantages that we propose, we made homogeneous multicolor QD-encoded microspheres to investigate stability and accuracy of fluorescence encoding by the self-healing encapsulation strategy. The feasibility was demonstrated by using orange and red QDs with emission peaking at 591 and 649 nm, respectively. The results are shown in Figure 6a1−a3 demonstrate that composite beads simultaneously incorporate that the two types of QDs show an emission profile mainly determined by their input ratio and no fluctuations in wavelength are found. Figure 5a4 shows the statistical distribution of 591 nm/655 nm ratiometric measurements of the three simple barcode preparations, where the ratios of the relative fluorescence intensities (1:5, 1:1, 12:5) are plotted as a histogram, each for 200 beads. The relative standard deviation of each distribution is 6.7%, 2.3%, and 7.3% for median relative intensity levels of 0.19, 0.98, and 2.37, respectively. The results demonstrate tiny fluctuations of the absolute intensity from bead to bead fabricated by the self-healing encapsulation strategy, indicating that the self-healing encapsulation strategy could achieve steadily and accurate encoding.

3.3. Activity of Surface Groups−Carboxyl Groups and Immunoreactions. Besides optical encoding, surface functional groups are also vital to the applications of QD-encoded microspheres. In our experiment, porous polymer microspheres are the carriers of QD-encoded fluorescent microspheres, whose surface functional groups−carboxyl groups can be used as sites for the attachment of DNA sequence, antigen, or antibody via well-established carbodiimide chemistry. The applicability of these fluorescent microspheres as suspension array was examined in a sandwich immunoassay for AFP (see Figure 7). In this study, AFP capture antibody are tagged onto the surface of QD-encoded microspheres via amide bond formation between the carboxyl groups on the bead surface and the primary amine groups of the protein and BSA are attached onto microspheres as nonspecific binding control. If antigens are immobilized on the QD-encoded microspheres, the FITC-labeled AFP reporter body could be captured by antigen. Fluorescence intensities are measured after the corresponding FITC-labeled AFP reporter antibody is added. Here, the emission wavelength of QD-encoded microspheres is 591 nm which can be measured on the FL3 channel (PE-TR channel) for decoding of encoded beads and the fluorescent intensities of all samples on FL3 channel are constant. The FITC fluorescence signal was measured on the FL1 channel for the decoding of FITC-labeled AFP reporter antibody. After immunoreactions, the signal intensity in the FL1 channel between the BSA control group and AFP group appear significantly different; the intensity of the AFP group in FL1 is higher than the BSA control group, indicating that the immunoreactions between QD-encoded fluorescent microspheres/antigens and antibodies really occur on the surface of fluorescent microspheres in this study. The results can be confirmed by the activity of carboxyl groups on the surface of

the QD-encoded microspheres and indicates that the immunoreactions between QD-encoded fluorescent microspheres/antigens and antibodies really occurred on the surface of fluorescent microspheres in this study.

4. CONCLUSIONS

In conclusion, we presented a new self-healing encapsulation strategy to generate functionalized uniform quantum-dot barcodes with high physical and chemical stability. This efficient and facile formulation could make porous polymer microspheres self-heal to encapsulate QDs via the thermal motion and interaction of the molecular chain. Compared with the traditional QD-encoded microspheres with unsealed pores, the new strategy solved especially the QD leakage problem and improved the chemical stability under different pH physiological conditions as well as the longtime storage stability. In the meantime, quantum-dot encoding capacity and the spatial distribution uniformity could be also improved. The statistical distribution of 591 nm/655 nm ratiometric measurements in multicolor barcodes indicates that the self-healing encapsulation strategy could achieve steady and accurate option encoding. Furthermore, immunoassay performance for AFP detections indicates that carboxyl groups on the fluorescence microsphere surface facilitate efficient attachment of the biomacromolecule.

■ ASSOCIATED CONTENT

Ⓢ Supporting Information

Spectra of the quantum-dot barcodes by self-healing encapsulation and (inset) the corresponding fluorescence images. Fluorescence image of QD-encoded microspheres with various QD concentration and corresponding relationship curves. This material is available free of charge via the Internet at http://pubs.acs.org.

■ AUTHOR INFORMATION

Corresponding Authors

*Tel. and fax: +86-022-27401821. E-mail: jinchang@tju.edu.cn
*E-mail: xuanlx@hotmail.com.

Author Contributions

⊥T.S. and J.L. had equal contribution to this paper.

Notes

The authors declare no competing financial interest.

■ ACKNOWLEDGMENTS

The authors gratefully acknowledge National High Technology Program of China (863 Program) (2012AA022603), Nature Science Foundation of China (51373117), Key Project of Tianjin Applied Basic Research Program (13JCZDJC33200), and Doctoral Base Foundation of Educational Ministry of China (20120032110027).

■ REFERENCES

(1) Pregibon, D. C.; Toner, M.; Doyle, P. S. *Science* **2007**, *315*, 1393−1396.
(2) Birtwell, S.; Morgan, H. *Integr. Biol.* **2009**, *1*, 345−362.
(3) Lin, C.; Jungmann, R.; Leifer, A. M.; Li, C.; Levner, D.; Church, G. M.; Shih, W. M.; Yin, P. *Nature Chem.* **2012**, *4*, 832−839.
(4) Nolan, J. P.; Sklar, L. A. *Trends Biotechnol.* **2002**, *20*, 9−12.
(5) Wilson, R.; Cossins, A. R.; Spiller, D. G. *Angew. Chem., Int. Ed.* **2006**, *45*, 6104−6117.
(6) Broder, G. R.; Ranasinghe, R. T.; She, J. K.; Banu, S.; Birtwell, S. W.; Cavalli, G.; Galitonov, G. S.; Holmes, D.; Martins, H. F.; MacDonald, K. F. *Anal. Chem.* **2008**, *80*, 1902−1909.
(7) Zhao, X.; Cao, Y.; Ito, F.; Chen, H. H.; Nagai, K.; Zhao, Y. H.; Gu, Z. Z. *Angew. Chem., Int. Ed.* **2006**, *45*, 6835−6838.
(8) Zhao, Y.; Zhao, X.; Sun, C.; Li, J.; Zhu, R.; Gu, Z. *Anal. Chem.* **2008**, *80*, 1598−1605.
(9) Zhi, Z.-l.; Morita, Y.; Hasan, Q.; Tamiya, E. *Anal. Chem.* **2003**, *75*, 4125−4131.
(10) Braeckmans, K.; De Smedt, S. C.; Roelant, C.; Leblans, M.; Pauwels, R.; Demeester, J. *Nat. Mater.* **2003**, *2*, 169−173.
(11) Yang, C.; Zhong, Z.; Lieber, C. M. *Science* **2005**, *310*, 1304−1307.
(12) Han, M.; Gao, X.; Su, J. Z.; Nie, S. *Nat. Biotechnol.* **2001**, *19*, 631−635.
(13) Gao, X.; Nie, S. *J. Phys. Chem. B* **2003**, *107*, 11575−11578.
(14) Gao, X.; Nie, S. *Anal. Chem.* **2004**, *76*, 2406−2410.
(15) Sathe, T. R.; Agrawal, A.; Nie, S. *Anal. Chem.* **2006**, *78*, 5627−5632.
(16) Li, J.; Zhao, X.-W.; Zhao, Y.-J.; Gu, Z.-Z. *Chem. Commun.* **2009**, 2329−2331.
(17) Kuang, M.; Wang, D.; Bao, H.; Gao, M.; Möhwald, H.; Jiang, M. *Adv. Mater.* **2005**, *17*, 267−270.
(18) Vaidya, S. V.; Gilchrist, M. L.; Maldarelli, C.; Couzis, A. *Anal. Chem.* **2007**, *79*, 8520−8530.
(19) Rauf, S.; Glidle, A.; Cooper, J. M. *Adv. Mater.* **2009**, *21*, 4020−4024.
(20) Song, F.; Tang, P. S.; Durst, H.; Cramb, D. T.; Chan, W. C. *Angew. Chem.* **2012**, *124*, 8903−8907.
(21) Yang, Y.; Wen, Z.; Dong, Y.; Gao, M. *Small* **2006**, *2*, 898−901.
(22) Joumaa, N.; Lansalot, M.; Théretz, A.; Elaissari, A.; Sukhanova, A.; Artemyev, M.; Nabiev, I.; Cohen, J. H. *Langmuir* **2006**, *22*, 1810−1816.
(23) Wang, G.; Leng, Y.; Dou, H.; Wang, L.; Li, W.; Wang, X.; Sun, K.; Shen, L.; Yuan, X.; Li, J. *ACS Nano* **2012**, *7*, 471−481.
(24) Allen, C. N.; Lequeux, N.; Chassenieux, C.; Tessier, G.; Dubertret, B. *Adv. Mater.* **2007**, *19*, 4420−4425.
(25) Hu, S. H.; Gao, X. *Adv. Funct. Mater.* **2010**, *20*, 3721−3726.
(26) Chen, K.; Chou, L. Y.; Song, F.; Chan, W. C. *Nano Today* **2013**, *8*, 228−234.
(27) Song, T.; Zhang, Q.; Lu, C.; Gong, X.; Yang, Q.; Li, Y.; Liu, J.; Chang, J. *J. Mater. Chem.* **2011**, *21*, 2169−2177.
(28) Bae, W. K.; Char, K.; Hur, H.; Lee, S. *Chem. Mater.* **2008**, *20*, 531−539.
(29) Cui, Y.; Gong, X.; Zhu, S.; Li, Y.; Su, W.; Yang, Q.; Chang, J. *J. Mater. Chem.* **2011**, *22*, 462−469.
(30) Fleming, M. S.; Mandal, T. K.; Walt, D. R. *Chem. Mater.* **2001**, *13*, 2210−2216.
(31) Ottewill, R.; Schofield, A.; Waters, J.; Williams, N. S. J. *Colloid Polym. Sci.* **1997**, *275*, 274−283.
(32) Zhang, Y.; Broekhuis, A. A.; Picchioni, F. *Macromolecules* **2009**, *42*, 1906−1912.
(33) Desai, K.-G. H.; Schwendeman, S. P. *J. Controlled Release* **2013**, *165*, 62−74.
(34) Reinhold, S. E.; Desai, K. G. H.; Zhang, L.; Olsen, K. F.; Schwendeman, S. P. *Angew. Chem., Int. Ed.* **2012**, *51*, 10800−10803.